This article has been accepted for publication in a future proceedings of this conference, but has not been fully edited. Content may change prior to final publication.
Citation information: DOI: 10.1109/sampta64769.2025.11133533, 2025 International Conference on Sampling Theory and Applications (SampTA)

Parameter Selection in Complex-Valued Two-Channel Modulo ADC Sampling System

Wenyi Yan[1] Ruixiang Zhu[2] Zeyuan Li[3] Lu Gan[1] Hongqing Liu[4]
[1]Dept. of Electrical and Electronic Engineering, Brunel University, London, UK
[2]Dept. of Electrical and Electronic Engineering, University College London, London, UK
[3]Indium Engine Co., Ltd, Dongguan, China
[4]School of Communication and Information Engineering,
Chongqing University of Posts and Telecommunications, Chongqing, China

***Abstract*—Modulo Analog-to-digital converters (ADCs) extend the dynamic range of conventional ADCs by folding input signals, enabling the acquisition of signals beyond traditional limits. This paper presents two approaches for parameter selection in conjugate complex-valued 2-channel modulo ADC systems to improve error tolerance. The first is a closed-form sub-optimal method, which offers a near-optimal solution, making it suitable for efficiency-sensitive applications. The second is an effective search-based method that identifies the exact optimal solution with relatively low computational cost. Simulations show that the sub-optimal method provides performance close to the optimal solution, while the search-based method achieves precise optimisation with manageable computational requirements.**

***Index Terms*—Modulo samplers, Analog-to-digital converters, Number theory, Chinese remainder theorem, Gaussian integers.**

I. Introduction

Conventional analog-to-digital converters (ADCs) reach saturation when the input signal exceeds the threshold $\frac{\Delta}{2}$, constraining the output to $\left[-\frac{\Delta}{2}, \frac{\Delta}{2}\right]$, where $\Delta > 0$ is the peak-to-peak ADC range. Modulo ADCs mitigate the saturation issue by folding the input signal back into the range Δ, mathematically defined for $x \in \mathbb{R}$ as [1], [2]:

$$\langle x \rangle_{\Delta} = \Delta \left(\left[\!\!\left[\frac{x}{\Delta} + \frac{1}{2} \right]\!\!\right] - \frac{1}{2} \right), \quad [\![x]\!] \stackrel{\text{def}}{=} x - \lfloor x \rfloor$$

where $\lfloor \cdot \rfloor$ denotes the floor operation. The use of a single modulo ADC for sampling often leads to increased data volumes, higher storage requirements, and greater computational costs due to the high sampling rates required [3]–[6]. To mitigate these challenges, multi-channel modulo-ADC systems have been proposed [7]–[9], using an L-channel framework with progressively increasing ADC ranges $\Delta_1 < \Delta_2 < \cdots < \Delta_L \leq \Delta_{\max}$, defined as $\Delta_l = \epsilon \tau_l \quad \text{for} \quad 1 \leq l \leq L$, where ϵ is a positive real number related to system error tolerance, and τ_l represents co-prime integers. Signal reconstruction is accomplished through the robust Chinese remainder theorem (RCRT) [10]–[14], which ensures fast and reliable recovery. Stability is maintained when the maximum remainder error $\|\boldsymbol{e}\|_{\infty}$ from the samplers stays within the error bound δ, defined as $\|\boldsymbol{e}\|_{\infty} < \delta = \epsilon/4$.

While modulo ADCs explore many real-world applications—such as radar, imaging, and communications—these often involve processing complex-valued signals [15]–[22]. Traditionally, such signals are separated into real and imaginary components, $g(t) = \text{Real}[g(t)] + i\text{Imag}[g(t)]$, where $\text{Real}[g(t)]$ and $\text{Imag}[g(t)]$ are the real and imaginary components, with each part handled using separate thresholds. This method increases system complexity and hardware requirements. To address this, research has begun exploring the direct processing of complex-valued signals within complex-valued multi-channel modulo ADC frameworks [8].

While prior research focuses on optimising real-valued thresholds in modulo ADCs, no work has addressed parameter selection for complex-valued systems [9]. This paper fills this gap by proposing sub-optimal and optimal methods for selecting system parameters in conjugate complex-valued 2-channel modulo ADCs to maximise error bounds.

The paper is organised as follows: Section II reviews the 2-channel complex-valued modulo ADC system. Section III presents the random selection, closed-form sub-optimal selection, and search-based optimal selection methods for complex moduli. Section IV compares these selection methods, and Section V discusses results and future research directions.

Notations: In this paper, $i = \sqrt{-1}$ denotes the imaginary unit. For any complex signal, $g_{\max}$ is the maximum amplitude, defined as $g_{\max} = \max\{\|\text{Real}[g(t)]\|_{\infty}, \|\text{Imag}[g(t)]\|_{\infty}\}$. $\mathbb{Z}$ represents the set of integers, and $\mathbb{Z}[i]$ the Gaussian integers (complex numbers with integer real and imaginary parts). For $\pi_n = a + bi$, $\overline{\pi_n} = a - bi$ is the complex conjugate. $\mod$ denotes the standard modulo operation, where the result is always non-negative (e.g., $-1 \mod 4 = 3$), distinct from the fold operation in Eq. (1). $\lceil \cdot \rceil$ denotes the ceiling function.

II. Literature Review

In this section, we review the complex-valued 2-channel modulo ADC sampling system. For a complex number x, its complex modulo sampler is defined as [23]:

$$\langle x \rangle_{\Delta} = \Delta \left(\left[\!\!\left[\frac{x}{\Delta} + \frac{(1+i)}{2} \right]\!\!\right] - \frac{(1+i)}{2} \right)$$

where $[\![x]\!] \stackrel{\text{def}}{=} x - (\lfloor \text{Real}(x) \rfloor + i \lfloor \text{Imag}(x) \rfloor)$. The threshold Δ is now extended from real to complex values, defined as $\Delta = \epsilon\tau = \epsilon(a + bi)$, where ϵ is a real number representing

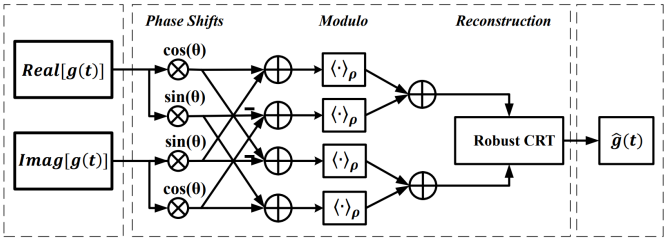

Fig. 1. Conjugate complex-valued 2-channel modulo ADC sampling system, where $\theta = \arctan\left(\frac{q}{p}\right)$ and $\rho = \epsilon\sqrt{p^2+q^2}$.

the system's error bound. In previous sections, τ was real-valued; here, it is a complex Gaussian integer with components a and b ($a, b \in \mathbb{Z}$). The norm of τ is $N(\tau) = |\tau|^2 = \tau\bar{\tau} = a^2 + b^2$ [24]. In a complex-valued 2-channel modulo ADC system, the complex thresholds are defined as:

$$\Delta_1 = \epsilon\tau_1 = \epsilon(p+qi), \quad \Delta_2 = \epsilon\tau_2 = \epsilon(p-qi) \tag{1}$$

where $p, q \in \mathbb{Z}$ and $|\Delta_1| = |\Delta_2| \leq \Delta_{\max}$. For RCRT-based reconstruction [10], the conjugate Gaussian integers $\tau_1 = p+qi$ and $\tau_2 = p-qi$ must be co-prime, satisfying [8], [25], [26]:

$$\gcd(p, q) = 1 \quad \text{and} \quad |p-q| \mod 2 = 1 \tag{2}$$

Lemma 1 below provides the method for computing the maximum recoverable signal range P and the corresponding error bounds δ for conjugate complex-valued moduli pairs.

Lemma 1. *In a complex-valued 2-channel modulo ADC system, let $\Delta_1 = \epsilon(p+iq)$ and $\Delta_2 = \epsilon(p-iq)$, where p and q are integers satisfying the coprimality condition in Eq. (2), and ϵ is a positive real number. The maximum recoverable peak-to-peak value P is given by $P = \frac{\epsilon(p^2+q^2)}{2}$, with the corresponding error bound $\delta = \frac{\epsilon}{4}$ [8].*

Figure 1 illustrates the complex-valued 2-channel modulo sampling system. The modulo operation applies phase shifts of $-\theta$ and θ, where $\theta = \arctan\left(\frac{q}{p}\right)$, to the real and imaginary components. The system uses a **unified** dynamic range $\rho = \epsilon\sqrt{p^2+q^2}$, eliminating the need for separate thresholds for each modulo ADCs. Managing multiple thresholds significantly increases hardware complexity and cost due to the added comparators and control circuits [27]–[29]. By contrast, the unified range in this complex-valued approach reduces hardware demands, resulting in a more efficient design [8]. Reconstruction of the complex modulo samples is performed using the RCRT [10].

III. Parameter Selection

In this section, we aim to improve the error bound δ by selecting the optimal threshold parameter, given the maximum input signal $g_{\max}$ and the maximum ADC range $\Delta_{\max}$.

A. Problem Formulation

Consider a 2-channel sampling system with thresholds Δ_1 and Δ_2, as defined in Eq. (1). The objective is to maximise ϵ through the appropriate selection of p and q, subject to the constraints imposed by $\Delta_{\max}$ and $g_{\max}$. This problem is governed by the following two conditions:

$$\begin{aligned} |\Delta_1| = |\Delta_2| &= \epsilon\sqrt{p^2+q^2} \leq \Delta_{\max} \\ P &= \frac{\epsilon(p^2+q^2)}{2} > g_{\max} \end{aligned} \tag{3}$$

Defining $\gamma = \sqrt{p^2+q^2}$, the first inequality in Eq. (3) imposes $\epsilon \leq \frac{\Delta_{\max}}{\gamma}$, while the second condition requires $\epsilon > \frac{2g_{\max}}{\gamma^2}$. From these two inequalities, we can determine that ϵ is bounded by $\frac{2g_{\max}}{\gamma^2} < \epsilon \leq \frac{\Delta_{\max}}{\gamma}$. Further simplification yields $\frac{\Delta_{\max}}{\gamma} > \frac{2g_{\max}}{\gamma^2}$, which leads to the condition

$$\gamma > \frac{2g_{\max}}{\Delta_{\max}}. \tag{4}$$

To maximise ϵ, the relation $\epsilon = \frac{\Delta_{\max}}{\gamma}$ suggests that ϵ increases as γ approaches $\frac{2g_{\max}}{\Delta_{\max}}$. Consequently, the optimal choice is a co-prime pair (p, q) such that γ is as close as possible to this value.

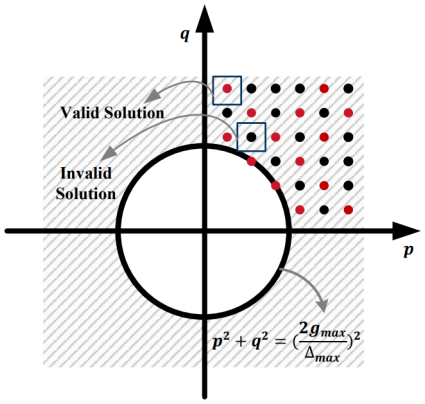

Fig. 2. Illustration of parameter selection, focusing on identifying co-prime integer points outside the circle defined by $\gamma > \frac{2g_{\max}}{\Delta_{\max}}$.

As illustrated in Figure 2, the circle defined by $p^2+q^2 = \left(\frac{2g_{\max}}{\Delta_{\max}}\right)^2$ serves as the boundary for selecting p and q. Black dots represent integer points outside the circle, while red dots indicate co-prime integer pairs with different parities. The goal is to identify the nearest red dot to the circle, which corresponds to the optimal parameter pair, thereby maximising ϵ within the given constraints.

B. Parameter Selection

Having established the problem formulation, we now explore several methods for selecting the integer values of p and q that satisfy the given constraints in Eq. (3). The first method relies on a random selection process, followed by more systematic approaches, including an analytical formula and a simplified search algorithm.

1) Random Selection: To determine integer values for p and q, we begin with $\beta = \frac{2g_{\max}}{\Delta_{\max}}$ and randomly select an angle $\theta \in (0, \frac{\pi}{2}]$ to ensure both p and q are positive. Since only $\sqrt{p^2+q^2}$ is relevant, selecting θ from the first quadrant suffices. The integer values of p and q are then computed as $p = \lceil \beta\cos(\theta) \rceil$ and $q = \lceil \beta\sin(\theta) \rceil$. We then verify whether

Algorithm 1 Random Selection

Input: $g_{\max}$, $\Delta_{\max}$
Output: p, q, and γ
Initialize $\beta = \frac{2g_{\max}}{\Delta_{\max}}$
repeat
  Uniformly at random select $\theta \in [0, \frac{\pi}{2}]$
  Compute $p = \lceil \beta \cos(\theta) \rceil$, $q = \lceil \beta \sin(\theta) \rceil$
  if $\gcd(p, q) = 1$ and $|p - q| \mod 2 = 1$, **then**
    Compute $\gamma = \sqrt{p^2 + q^2}$
    return p, q, and γ
  end if
until p and q meet the condition in Eq. (2)

p and q are co-prime using Eq. (2). If not, the selection is discarded; otherwise, we compute $\gamma = \sqrt{p^2 + q^2}$ and check how closely γ approximates β. Algorithm 1 outlines the random selection process.

Note that this random search algorithm may not be efficient. For example, if $\beta = 7$ and $\theta = 0.6$, we calculate $p = 6$ and $q = 4$. Since $\gcd(6, 4) = 2$, the pair is not co-prime and fails to meet the condition in Eq. (2), illustrating the inefficiency of random selection, which may require multiple attempts to find valid pairs. Similarly, for $\beta = 7$ and $\theta = 0.3$, we get $p = 5$ and $q = 2$. Although this pair satisfies the co-prime condition ($\gcd(5, 2) = 1$), the value $\sqrt{p^2 + q^2} - \beta \approx 1.39$ shows that it is not close to optimal.

2) Sub-Optimal Selection: We now turn to a more structured method for selecting p and q based on theoretical analysis. Corollary 1 provides the closed-form sub-optimal selection of p and q, derived to satisfy the constraints in Eq. (3) and ensure reliable signal reconstruction.

Corollary 1. *Given the maximum ADC threshold Δ_{max} and the maximum input signal g_{max}, for a complex-valued 2-channel modulo ADC system with $\Delta_1 = \epsilon(p+iq)$ and $\Delta_2 = \epsilon(p-iq)$, the sub-optimal selection is given by:*

$$p = \left\lceil \frac{2g_{max}}{\Delta_{max}} \right\rceil, \quad q = \begin{cases} 1, & \text{if } p \text{ is even} \\ 2, & \text{if } p \text{ is odd} \end{cases} \qquad \epsilon = \frac{\Delta_{max}}{\sqrt{p^2 + q^2}} \tag{5}$$

Proof. To ensure reliable reconstruction and optimal error tolerance, the recoverable peak-to-peak value P must satisfy $P = \frac{\Delta_{\max}\sqrt{p^2+q^2}}{2} \geq g_{\max}$. Given that the error tolerance ϵ is defined as $\epsilon = \frac{\Delta_{\max}}{\sqrt{p^2+q^2}}$, maximising ϵ requires minimising p and q. Thus, we set $p = \left\lceil \frac{2g_{\max}}{\Delta_{\max}} \right\rceil$. To ensure p and q are co-prime with differing parity, we choose $q = 1$ if p is even, and $q = 2$ if p is odd. ∎

The closed-form sub-optimal selection provides a near-optimal solution that satisfies system requirements while simplifying the selection process. Although not strictly optimal, this method effectively balances computational efficiency with reliable signal reconstruction, mitigating the inefficiencies of random selection.

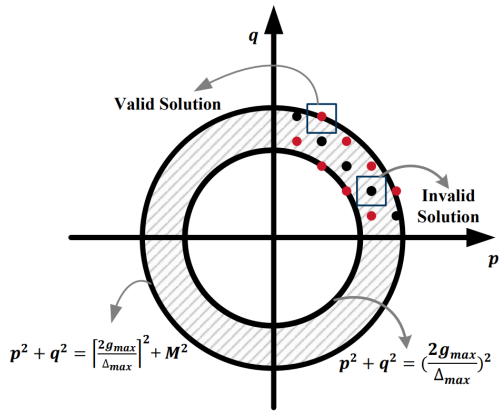

Fig. 3. Optimal parameter selection for complex-valued 2-channel modulo ADCs.

3) Search-Based Optimal Selection: Based on the previous discussion, the lower bound of p^2+q^2 is given in Eq. (4), while Corollary 1 defines a sub-optimal upper bound. By combining these with number-theoretic methods, we establish an effective search-based optimal selection approach.

Figure 3 illustrates this optimal selection principle. The black dots represent integer pairs that do not satisfy Eq. (2), while the red dots indicate valid pairs between the inner and outer circles. The goal is to find the red dot closest to the inner circle, maximising ϵ while ensuring that $p^2 + q^2$ lies within the defined bounds:

$$\left(\frac{2g_{\max}}{\Delta_{\max}}\right)^2 \leq p^2 + q^2 \leq \left(\left\lceil \frac{2g_{\max}}{\Delta_{\max}} \right\rceil\right)^2 + M^2 \tag{6}$$

where $M = 1$ if $\left\lceil \frac{2g_{\max}}{\Delta_{\max}} \right\rceil$ is even, and $M = 2$ if it is odd.

To efficiently identify the optimal pair (p, q), we leverage number-theoretic properties of sums of squares as presented in the following Corollary 2 [30]. Note that in the explanation below, " mod " refers to the standard modulo operation.

Corollary 2. *Let $N = p^2+q^2$. Then, p and q satisfy Eq. (2) if and only if all prime factors of N are congruent to $1 \pmod 4$.*

The proof of the above Corollary follows from Fermat's Two Squares Theorem [30]–[32]. Due to space limitations, the proof is omitted here, but a more detailed explanation will be provided in a forthcoming journal paper.

Our objective is to find the minimal $N = p^2+q^2$ within the bounds specified in Eq. (6), starting with $N = \left\lceil \left(\frac{2g_{\max}}{\Delta_{\max}}\right)^2 \right\rceil$. To ensure N can be written as $N = p^2 + q^2$, with p and q having different parity, we adjust it to satisfy $N \equiv 1 \pmod 4$ by applying $N = N + (1 - (N \mod 4)) \mod 4$ Then, to ensure that p and q are co-prime, we first factor N as $N = \prod_{n=1}^{m} r_n^{k_n}$, confirming that all prime factors satisfy $r_n \equiv 1 \pmod 4$. Each r_n is then decomposed into a Gaussian prime π_n and its conjugate $\overline{\pi_n}$, as $r_n = \pi_n\overline{\pi_n}$. We select one factor

Algorithm 2 Search-based Optimal Selection

Input: $g_{\max}$, $\Delta_{\max}$
Output: Optimal p_{opt} and q_{opt}
Compute Upper Bound $= \left(\left\lceil \frac{2g_{\max}}{\Delta_{\max}} \right\rceil \right)^2 + M^2$
Initialize $N \leftarrow \left\lceil \left(\frac{2g_{\max}}{\Delta_{\max}} \right)^2 \right\rceil$
Compute $N = N + (1 - (N \mod 4)) \mod 4$
While $N \leq$ Upper Bound
    Factorize N as $N = \prod_{n=1}^{m} r_n^{k_n}$, where r_n are distinct primes and k_n are natural integers.
    If $r_n \equiv 1 \pmod 4$ for all $1 \leq n \leq m$
        Factor r_n in $\mathbb{Z}[i]$ as $r_n = \pi_n \overline{\pi_n}$, where π_n is a prime Gauss integer and $\overline{\pi_n}$ is its conjugate.
        Compute $\alpha = \prod_{n=1}^{m} \pi_n^{k_n}$
        Return $p_{\text{opt}} = \text{Real}(\alpha)$ and $q_{\text{opt}} = \text{Imag}(\alpha)$.
    Else
        $N \leftarrow N + 4$
End While

from each conjugate pair to construct $\alpha = \prod_{n=1}^{m} \pi_n^{k_n} = p + iq$. This pair of p and q provide the optimal selection. If any r_n does not satisfy $r_n \equiv 1 \pmod 4$, we increment N by 4 and repeat the process. Algorithm 2 provides a detailed description of search-based optimal selection. Here, all factorizations into prime (Gauss) integers can be easily obtained using software packages such as SageMath [33].

IV. Simulation results

In this section, we assess the performance of various parameter selection methods, including the random search approach, the sub-optimal selection derived from Corollary 1, and the search-based optimal selection.

With $\Delta_{\max} = 25$ and $g_{\max}$ set to 160, 225, and 385, corresponding to β values of 12.8, 18, and 30.8, respectively, 10,000 random trials were conducted. In each trial, $\theta \in (0, \frac{\pi}{2}]$ was selected uniformly at random, and $p = \lceil \gamma \cos(\theta) \rceil$ and $q = \lceil \gamma \sin(\theta) \rceil$ were computed. The minimum and maximum recoverable dynamic ranges, P_{min} and P_{max}, were recorded, alongside P_{avg}, denoting the average recoverable dynamic range across successful trials. Additionally, δ_{avg} was calculated to quantify the average error bound observed in these trials. The parameter d represents the distance from the lower boundary, $\beta = \frac{2g_{\max}}{\Delta_{\max}}$, defined as:

$$d = |\gamma - \beta| = \left| \sqrt{p^2 + q^2} - \beta \right| \tag{7}$$

Smaller values of d indicate closer proximity to the optimal design. The average distance is denoted as d_{avg}.

As shown in Table I, the success rates for identifying valid coprime pairs ranged from 33.4% to 57.8%. The low success rate underscores the inefficiency of the random search method, with d_{avg} indicating that the selected values of p and q in successful cases are not close to optimal.

TABLE I
Random Search Selection

β	Success Rate	$[P_{\min}, P_{\max}]$	P_{avg}	δ_{avg}	d_{avg}
12.8	57.8%	[162,173]	168	0.465	0.66
18	33.4%	[225,238]	231	0.337	0.54
30.8	33.8%	[385,399]	392	0.199	0.62

TABLE II
Comparison of Sub-optimal Selection and Optimal Selection

β	Selection Methods	p	q	P	δ	d
12.8	Sub-optimal Selection	13	2	164.4	0.475	0.35
	Optimal Selection	12	5	162.5	0.481	0.2
18	Sub-optimal Selection	18	1	225	0.347	0.02
	Optimal Selection	18	1	225	0.347	0.02
30.8	Sub-optimal Selection	31	2	388	0.201	0.26
	Optimal Selection	30	7	385	0.203	0.01

We evaluated the performance of the sub-optimal and optimal selections under the same parameter settings as in the random search experiments, with $\beta = 12.8$, 18, and 30.8. For each case, we computed p, q, recoverable dynamic range P, error bound δ, and deviation d for both methods. For $\beta = 12.8$ and $\beta = 30.8$, the optimal method exhibited a lower deviation (e.g., at $\beta = 12.8$, the optimal selection produced $d = 0.2$, compared to $d = 0.35$ for the sub-optimal selection). However, these differences were relatively minor when compared to the random selection, which showed a larger deviation ($d = 0.66$). Notably, for $\beta = 18$, the sub-optimal and optimal methods resulted in identical parameter values, yielding the same recoverable dynamic range and minimal deviation ($d = 0.02$).

These results demonstrate that the sub-optimal selection provides solutions that are close to the optimal selection. The search-based optimal selection efficiently finds the optimal solution with low computational cost.

V. Conclusion and Future Work

This paper addresses the challenge of parameter selection in complex-valued 2-channel modulo ADC systems, exploring random, sub-optimal, and search-based methods to maximise error tolerance. Simulation results demonstrate that the random selection method is likely to choose invalid threshold parameters with high probability, while the sub-optimal selection provides solutions close to the optimal selection. The search-based optimal selection efficiently finds the optimal solution with low computational cost.

In future work, we aim to implement these methods in hardware to validate their effectiveness in real-time applications.

REFERENCES

[1] Ayush Bhandari, Felix Krahmer, and Ramesh Raskar, "On Unlimited Sampling and Reconstruction," *IEEE Transactions on Signal Processing*, vol. 69, pp. 3827–3839, 2021, Conference Name: IEEE Transactions on Signal Processing.

[2] Ayush Bhandari, Felix Krahmer, and Ramesh Raskar, "On unlimited sampling," in *2017 International Conference on Sampling Theory and Applications (SampTA)*, July 2017, pp. 31–35.

[3] Ayush Bhandari, Felix Krahmer, and Ramesh Raskar, "Unlimited sampling of sparse signals," in *2018 IEEE International Conference on Acoustics, Speech and Signal Processing (ICASSP)*, 2018, pp. 4569–4573.

[4] Dorian Florescu and Ayush Bhandari, "Modulo event-driven sampling: System identification and hardware experiments," in *ICASSP 2022 - 2022 IEEE International Conference on Acoustics, Speech and Signal Processing (ICASSP)*, 2022, pp. 5747–5751.

[5] Ayush Bhandari, Felix Krahmer, and Ramesh Raskar, "Unlimited sampling of sparse sinusoidal mixtures," in *2018 IEEE International Symposium on Information Theory (ISIT)*, 2018, pp. 336–340.

[6] Elad Romanov and Or Ordentlich, "Above the Nyquist Rate, modulo folding does not hurt," *IEEE Signal Processing Letters*, vol. 26, no. 8, pp. 1167–1171, Aug. 2019.

[7] Lu Gan and Hongqing Liu, "High dynamic range sensing using multi-channel modulo samplers," *Proceedings of the IEEE Sensor Array and Multichannel Signal Processing Workshop*, vol. 2020-June, 6 2020.

[8] Yicheng Gong, Lu Gan, and Hongqing Liu, "Multi-channel modulo samplers constructed from gaussian integers," *IEEE Signal Processing Letters*, vol. 28, pp. 1828–1832, 2021.

[9] Wenyi Yan, Lu Gan, Shaoqing Hu, and Hongqing Liu, "Towards optimized multi-channel modulo-ADCs: Moduli selection strategies and bit depth analysis," in *ICASSP 2024 - 2024 IEEE International Conference on Acoustics, Speech and Signal Processing (ICASSP)*, Seoul, Korea, Republic of, Apr. 2024, pp. 9496–9500, IEEE.

[10] Wenjie Wang and Xiang-Gen Xia, "A closed-form robust Chinese remainder theorem and its performance analysis," *IEEE Transactions on Signal Processing*, vol. 58, no. 11, pp. 5655–5666, 2010.

[11] Xiaoping Li, Xiang-Gen Xia, Wenjie Wang, and Wei Wang, "A robust generalized chinese remainder theorem for two integers," *IEEE Transactions on Information Theory*, vol. 62, no. 12, pp. 7491–7504, 2016.

[12] Wenjie Wang, Xiaoping Li, Wei Wang, and Xiang-Gen Xia, "Maximum likelihood estimation based robust Chinese remainder theorem for real numbers and its fast algorithm," *IEEE Transactions on Signal Processing*, vol. 63, no. 13, pp. 3317–3331, 2015.

[13] Li Xiao, Xiang-Gen Xia, and Wenjie Wang, "Multi-stage robust Chinese remainder theorem," *IEEE Transactions on Signal Processing*, vol. 62, no. 18, pp. 4772–4785, 2014.

[14] Li Xiao and Xiang-Gen Xia, "Frequency determination from truly sub-nyquist samplers based on robust Chinese remainder theorem," *Signal Processing*, vol. 150, pp. 248–258, 2018.

[15] Thomas Feuillen, Mohammad Alaee-Kerahroodi, Ayush Bhandari, M. R. Bhavani Shankar, and Björn Ottersten, "Unlimited sampling for FMCW radars: A proof of concept," 2022, Institute of Electrical and Electronics Engineers.

[16] Hanbyol Jang, Kihun Bang, Jinseong Jang, and Dosik Hwang, "Dynamic range expansion using cumulative histogram learning for high dynamic range image generation," *IEEE Access*, vol. 8, pp. 38554–38567, 2020.

[17] Ayush Bhandari and Felix Krahmer, "HDR imaging from quantization noise," in *2020 IEEE International Conference on Image Processing (ICIP)*, 2020, pp. 101–105.

[18] Hao Shi, Qingqing Sheng, Yupei Wang, Bingying Yue, and Liang Chen, "Dynamic range compression self-adaption method for sar image based on deep learning," *Remote Sensing*, vol. 14, no. 10, pp. 2338, 2022.

[19] Thomas Feuillen, Bhavani Shankar MRR, and Ayush Bhandari, "Unlimited sampling radar: Life below the quantization noise," in *ICASSP 2023 - 2023 IEEE International Conference on Acoustics, Speech and Signal Processing (ICASSP)*, 2023, pp. 1–5.

[20] Danson Evan Garcia, Jesse Hernandez, and Steve Mann, "Automatic gain control for enhanced HDR performance on audio," in *2020 IEEE 22nd International Workshop on Multimedia Signal Processing (MMSP)*, 2020, pp. 1–6.

[21] K. Yamada, T. Nakano, and S. Yamamoto, "A vision sensor having an expanded dynamic range for autonomous vehicles," *IEEE Transactions on Vehicular Technology*, vol. 47, no. 1, pp. 332–341, 1998.

[22] Jelena Kocić, Nenad Jovičić, and Vujo Drndarević, "Sensors and sensor fusion in autonomous vehicles," in *2018 26th Telecommunications Forum (TELFOR)*, 2018, pp. 420–425.

[23] Václav Pavlícek, Ruiming Guo, and Ayush Bhandari, "Bits, channels, frequencies and unlimited sensing: Pushing the limits of sub-nyquist prony," *measurements {vl [n]}*, vol. 50, pp. I4.

[24] K. Conrad, "The gaussian integers," [Online], Available: https://kconrad.math.uconn.edu/math5230f12/handouts/Zinotes.pdf.

[25] Conghui Li, Lu Gan, and Cong Ling, "Coprime sensing via Chinese remaindering over quadratic fields - part II: Generalizations and applications," 6 2019, vol. 67, pp. 2911–2922, Institute of Electrical and Electronics Engineers Inc.

[26] Conghui Li, Lu Gan, and Cong Ling, "Coprime sensing via Chinese remaindering over quadratic fields - part I: Array designs," *IEEE Transactions on Signal Processing*, vol. 67, pp. 2898–2910, 6 2019.

[27] Adithya Krishna, Sunil Rudresh, Vishal Shaw, Hemanth Reddy Sabbella, Chandra Sekhar Seelamantula, and Chetan Singh Thakur, "Unlimited Dynamic Range Analog-to-Digital Conversion," Nov. 2019, arXiv:1911.09371 [eess].

[28] Satish Mulleti, Eliya Reznitskiy, Shlomi Savariego, Moshe Namer, Nimrod Glazer, and Yonina C. Eldar, "A hardware prototype of wideband high-dynamic range analog-to-digital converter," *IET Circuits, Devices & Systems*, vol. 17, no. 4, pp. 181–192, 2023, _eprint: https://onlinelibrary.wiley.com/doi/pdf/10.1049/cds2.12156.

[29] Ayush Bhandari, Felix Krahmer, and Thomas Poskitt, "Unlimited Sampling From Theory to Practice: Fourier-Prony Recovery and Prototype ADC," *IEEE Transactions on Signal Processing*, vol. 70, pp. 1131–1141, 2022.

[30] D. Zagier, "A One-Sentence Proof That Every Prime $p \equiv 1 \mod 4$ Is a Sum of Two Squares," *The American Mathematical Monthly*, vol. 97, no. 2, pp. 144–144, 1990, Publisher: [Taylor & Francis, Ltd., Mathematical Association of America].

[31] K. Ireland and M.I. Rosen, *A Classical Introduction to Modern Number Theory*, Graduate Texts in Mathematics. Springer, 1990.

[32] G. H. Hardy and E. M. Wright, *An Introduction to the Theory of Numbers*, Oxford, fourth edition, 1975.

[33] SageMath, Inc., "Sagemath, the sage mathematics software system (version 9.8)," https://www.sagemath.org/, 2024.